

**NASA TECHNICAL  
MEMORANDUM**

**NASA TM X-52434**

**NASA TM X-52434**

**GPO PRICE \$** \_\_\_\_\_

**CSFTI PRICE(S) \$** \_\_\_\_\_

**Hard copy (HC)** \_\_\_\_\_

**Microfiche (MF)** \_\_\_\_\_

ff 653 July 65

FACILITY FORM 602	<b>N 68-33996</b>	
	(ACCESSION NUMBER)	(THRU)
	<b>19</b>	<b>1</b>
	(PAGES)	(CODE)
	<b>TMX 52434</b>	<b>33</b>
	(NASA CR OR TMX OR AD NUMBER)	(CATEGORY)

**COMBUSTION OF HYDROGEN AND METHANE TO  
SIMULATE EXPANSION OF STORABLE PROPELLANTS**

by Robert Friedman, Raymond E. Gaugler, and Erwin A. Lezberg  
Lewis Research Center  
Cleveland, Ohio

**TECHNICAL PAPER** proposed for presentation at Fourth  
Propulsion Joint Specialist Conference sponsored by  
the American Institute of Aeronautics and Astronautics  
Cleveland, Ohio, June 10-14, 1968



**NATIONAL AERONAUTICS AND SPACE ADMINISTRATION • WASHINGTON, D.C. • 1968**

**COMBUSTION OF HYDROGEN AND METHANE TO SIMULATE  
EXPANSION OF STORABLE PROPELLANTS**

**by Robert Friedman, Raymond E. Gaugler, and Erwin A. Lezberg**

**Lewis Research Center  
Cleveland, Ohio**

**TECHNICAL PAPER proposed for presentation at  
Fourth Propulsion Joint Specialist Conference  
sponsored by the American Institute of Aeronautics and Astronautics  
Cleveland, Ohio, June 10-14, 1968**

**NATIONAL AERONAUTICS AND SPACE ADMINISTRATION**

# COMBUSTION OF HYDROGEN AND METHANE TO SIMULATE EXPANSION OF STORABLE PROPELLANTS

by Robert Friedman, Raymond E. Gaugler, and Erwin A. Lezberg

Lewis Research Center  
National Aeronautics and Space Administration  
Cleveland, Ohio

## Abstract

An experimental investigation of exhaust-nozzle temperatures for the storable system, 50 percent UDMH-50 percent hydrazine/nitrogen tetroxide, was conducted using hydrogen and methane fuel burned in oxygen-enriched air to provide the same atomic constituents as the storable propellants. Oxidant-fuel mass ratios of 1.6 to 2.5 at 3.7 atmospheres combustion-chamber pressure were simulated by control of the fuel, oxygen, and air flows; inlet enthalpies were duplicated by preheating the oxidant in a pebble-bed storage heater. Static temperatures, measured by a spectral line reversal pyrometer at 5 stations in the expanding portion of a 5.5-area-ratio, Mach 3 nozzle, were found to be nearly insensitive to oxidant-fuel ratio and close to temperatures calculated for a frozen expansion. This study demonstrated the feasibility of the simulation technique for exhaust-nozzle kinetic studies. Results agreed well with a simplified kinetic analysis based on a "sudden freezing" of the nozzle recombination reactions at an area ratio of 1.04 upstream of the throat.

## Introduction

The storable propellant system consisting of a 50 percent by weight mixture of hydrazine and unsymmetrical dimethylhydrazine (UDMH) fuel and nitrogen tetroxide oxidizer is used in many advanced rocket engines, and experimental performance of several space-vehicle engines, using this propellant system, has been reported.<sup>(1)</sup> The actual engine performance is degraded by combustion, aerodynamic, and kinetic losses. The latter result from the reduction in nozzle energy release due to the incomplete recombination of the atoms and free radicals formed during the high-temperature combustion. These chemical recombination reactions have finite reaction times, which are often slow with respect to the residence time of the exhaust products in the nozzle. The prediction of kinetic losses for the storable propellant system has been the subject of several papers<sup>(2,3,4)</sup>; it is desirable, however, to supplement these predictions, which are based on idealized laboratory reaction-rate data, with experimental measurements under conditions more closely approaching those encountered in rocket engine environments.

This paper reports experimental measurements of the expansion of the products of combustion of storable propellants in a 5.5-area ratio, nominal Mach 3 nozzle. The actual liquid propellants were not used, however; instead a mixture of hydrogen and natural gas (93.6 percent methane) was burned in preheated oxygen-enriched air. For a study concerned with kinetic losses, this technique makes it possible to duplicate the combustion-

chamber products and enthalpy of the desired storable-propellant system using gaseous propellants, eliminating combustor inefficiencies and instabilities. A recent report also suggests this method of simulation.<sup>(5)</sup>

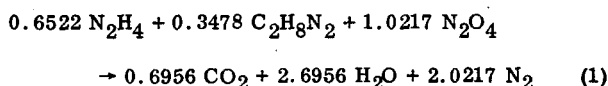
Experimental static temperatures are reported for the simulated storable propellants at a combustion-chamber pressure of 3.7 atmospheres, covering a range of oxidant-fuel weight ratios of 1.6 to 2.5 (equivalence ratios of 1.4 to 0.9). The experimental data are compared to analytical calculations based on theoretical equilibrium and kinetic expansions, and the application of the data to performance predictions of rocket engines is discussed.

## Simulation

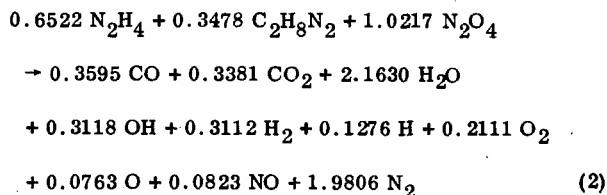
The simulation of one propellant system by another is defined here as the substitution of reactants which yield, upon combustion, the same products and mixture enthalpy as the desired system. The two gaseous combustion products at the same pressure are identical if their composition and enthalpy are equal.

## Composition

The combustion of 50 percent by weight hydrazine,  $N_2H_4$ , and unsymmetrical dimethyl hydrazine (UDMH),  $C_2H_5N_2$ , fuel with nitrogen tetroxide oxidizer,  $N_2O_4$ , (referred to hereafter as the storable, or liquid storable, propellant system) is written on the basis of one mole of fuel:

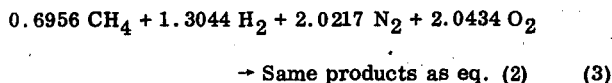


However, the combustion temperature of these propellants is about  $4130^\circ K$ , and the theoretical molecular products shown in equation (1) would be partly dissociated. An equilibrium calculation,<sup>(6)</sup> for example with liquid reactants at  $298^\circ K$  and 3.7 atmospheres, would show the following:

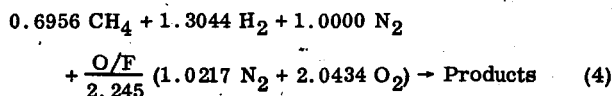


The endothermic dissociation reactions producing the atoms and free radicals would reduce the combustion temperature for this reaction to an equilibrium temperature of  $3045^\circ K$ . The simulation of the storable-

propellant composition therefore must provide reactants that produce the variety of products shown in equation (2). These products of combustion contain no compounds with N-H or C-H bonds, since the complex hydrazine and UDMH molecules are dissociated in the first steps of the reaction. Calculations thus show that a simple combination of methane, hydrogen, oxygen, and air, supplying the necessary C, H, O, and N atoms, would yield the same products as shown in equation (2), provided a means of duplicating enthalpy (or combustion temperature) were assured. Accordingly



To simulate the effects of operation over a range of oxidant-fuel mass ratios, equation (3) can be written



where O/F is the oxidant-fuel mass ratio (2.245 for stoichiometric combustion) and the products, not written out, would be a function of O/F, pressure, and enthalpy of the reactants. Note that, as required by equation (2), one mole of  $\text{N}_2$  is part of the fuel and the remainder part of the oxidant.

The experimental phase of this study used a mixture of 66.8 volume-percent hydrogen and 33.7 percent natural gas (93.6 percent methane) burned with air and oxygen to furnish the C, H, N, and O atoms required for simulation. The natural gas had a small percentage of ethane, higher hydrocarbons, and nitrogen, and these compounds were added to the reactants considered in equation (4). A typical fuel analysis is shown in table I.

### Enthalpy

The simulation of the enthalpy of the storable-propellant combustion products presents more difficulties; and, in a sense, the composition simulation cannot be treated separately from energy simulation, since the partly-dissociated products are a function of the combustion temperature. Table II lists the initial enthalpy values of the storable and simulated reactants, using values from Ref. 7 or data consistent with this source, based upon zero enthalpy at  $298.15^\circ \text{K}$  for reference elements. The enthalpy of  $\text{N}_2\text{O}_4$  assumes no dissociation to  $\text{NO}_2$  at the reactant conditions, but appendix B of Ref. 1 calculates that the influence of the neglect of the  $\text{NO}_2$  formation on the thermochemical or performance results is very small. The storable reactants have a higher initial enthalpy than that of the simulated reactants due to the heats of formation of hydrazine and UDMH. This energy is liberated in the combustion reaction and increases the enthalpy of the products. To compensate for this higher enthalpy of formation, the simulated reactants are preheated to increase their initial enthalpy. In this study, the preheating was more conveniently performed on the oxidants only, using an existing pebble-bed storage heater, and table II also lists oxidant enthalpies at  $950^\circ \text{K}$  for the

simulated propellants.

The desired match of combustion-product enthalpies was carried out by trial and error using a thermodynamic computer program.<sup>(6)</sup> Results are illustrated in Fig. 1, where combustion-product mixture enthalpy, using the same reference basis as table II, is shown as a function of the storable-propellant oxidant-fuel mass ratio. For the storable propellant, the product enthalpy decreases as the oxidant-fuel mass ratio increases since the proportion of low-initial-enthalpy reactant is increasing. For the simulated-propellant systems, represented at different oxidant-preheat levels by dashed curves in Fig. 1, the enthalpy-against-O/F trend is opposite to that of the storable propellants since in these cases increasing oxidant-fuel mass ratio increases the proportion of the high-initial-enthalpy reactant. The enthalpy simulation would be satisfied therefore by adjusting the oxidant-preheat temperature, covering the range of about  $1120^\circ$  to  $810^\circ \text{K}$  to correspond to the requirements for simulation of oxidant-fuel mass ratios of 1.6 to 2.5.

An example, comparing calculated properties of the storable-propellant and simulated-propellant products, is given in table III, which shows properties and compositions at the combustion chamber and at an exhaust-nozzle station where the products have expanded to 1/30 the combustion-chamber pressure, both for a fuel-rich O/F of 1.6. Nozzle compositions were calculated assuming an equilibrium expansion. To correspond to typical experimental conditions, the calculations were made with the simulated-propellant oxidant preheated to a nominal value of  $1100^\circ \text{K}$ , not quite the right match for the combustion-chamber enthalpy, and with the actual natural gas composition rather than pure methane. Nevertheless it is seen that the duplication of properties and composition can be controlled very closely.

### Apparatus

#### Installation

Air from the laboratory system and oxygen from a cylinder trailer were metered through standard orifices, heated in an aluminum-oxide, pebble-bed storage heat exchanger, passed through a water-cooled combustion chamber where the fuel mixture was introduced and ignited spontaneously, and expanded through a supersonic test nozzle. The combustion products were cooled and ducted to the laboratory exhaust system. Details of the storage heater and air flow system are given in Ref. 8.

The combustion chamber, nozzle, and typical instrumentation are shown in Fig. 2. The fuel was injected into the combustion chamber through water-cooled fuel-injection tubes arranged to cover approximately equal areas of the combustor cross-section. The combustion chamber itself was a cylindrical pipe, 30.7 cm in diameter and 46.5 cm long.

The test nozzle, similar to that described in Ref. 9, was a  $30^\circ$  half-angle converging,  $7^\circ$  diverging cone with a 17.7 cm radius-of-curvature throat. The throat inside diameter was 7.94 cm, and the diverging section was 46.7 cm long. Effective area ratio of the nozzle

was 5.5, corrected for boundary layer growth as determined by heated-air, nonburning calibrations. The nozzle had 5 pairs of nitrogen-purged, 1.3-cm-diameter optical ports located at diverging area ratios of 1.30, 1.65, 2.05, 2.50, and 3.60. Static-pressure taps were drilled normal to the nozzle wall, and wall thermocouples were mounted flush with the inside wall.

#### Spectral-Line Reversal Pyrometer

Static temperatures of the flowing exhaust gases in the test nozzle were measured using a self-balancing line reversal pyrometer.<sup>(10,11)</sup> The combustion products were seeded with sodium carbonate powder introduced by a water-cooled injector located in the combustion chamber, and a reversal temperature was measured by automatically balancing the seeded-gas radiation with that of a current-controlled tungsten-ribbon lamp mounted at the opposite optical window from a photomultiplier detector. Temperatures were computed from an initial calibration of the lamp brightness temperature as a function of lamp current, using an optical pyrometer. The pyrometer detector, lamp, and optics were mounted on an external U-shaped platform that straddled the test nozzle. The platform was moved to each of the optical port locations during a test run.

Optical ports were also located in the combustion chamber for initial measurements of combustion-chamber temperature profiles. The tungsten-ribbon lamp was replaced by a carbon arc reference source for higher reference temperatures,<sup>(10)</sup> and profiles were recorded by traversing the sodium carbonate injector across the combustion-chamber diameter and recording temperature as a function of radius.

#### Procedure

The simulation of the liquid storable propellants at desired oxidant-fuel mass ratios required three controls: (1) the composition of the fuel mixture, (2) the relative rates of fuel, oxygen, and air mass flows, and (3) the correct preheat of the oxidant mixture. The hydrogen and natural gas fuels were purchased from a commercial source, mixed, and stored at high pressure in a cylinder trailer with enough capacity for two to four complete test runs. The fuel mixture was analyzed by a mass spectrometer, and this analysis was used as a basis for calculating a table of values of relative fuel, oxygen, and air mass flows to simulate an O/F range of approximately 1.6 to 2.5, in accordance with equation (4) written for the exact fuel analysis. This O/F range was limited by the maximum possible fuel flow rate at one extreme and maximum oxygen flow rate at the other, but it encompassed the O/F values of interest to rocket engines. Tests were conducted at a single combustion-chamber pressure of 3.7 atmospheres. The air mass flow rate was thus a quantity fixed by the stagnation conditions, and the O/F settings were prescribed by values of the fuel-air and oxygen-air mass flow ratios. These ratios were regulated within  $\pm 2$  percent by an automatic control system, which adjusted the flow-valve openings using the ratio of differential pressures across fuel and oxygen flow orifices to the differential pressure across the air flow orifice. The oxidant-inlet temperature was controlled by the banking temperature, or the tempera-

ture maintained by the storage heater between run periods, and to a lesser extent by the length of the test runs. Experimental runs were conducted with the oxidant preheated to temperatures between 880° and 1120° K, approximately the range specified in Fig. 1 for correct enthalpy simulation. However, each series of runs at several different oxidant-fuel mass ratios was carried out at nearly constant oxidant-inlet temperatures, since it was not possible to vary the storage heater temperature as desired once air flow was established. Hence, the oxidant preheat temperature did not necessarily correspond to that required for enthalpy simulation. It will be shown that negligible changes in the exhaust-nozzle static temperatures are introduced by this compromise.

Nozzle static temperatures were measured by successively centering the reversal pyrometer on each optical window and recording the output on a strip-chart recorder. A complete survey, covering all five nozzle optical stations, took 4 to 5 minutes, during which time the oxidant-inlet temperature measured by a single shielded, platinum/platinum-13-percent-rhodium thermocouple varied no more than 20° K.

#### Analysis

##### Data Reduction

The treatment of experimental data consisted of (1) calculation of static temperatures from lamp-current readings of the reversal pyrometer, (2) calculation of flow rates and combustor-inlet temperatures, and (3) calculation of simulated oxidant-fuel ratios. The static temperature was hand calculated from a prior calibration of the reversal pyrometer, and flow rates and inlet temperatures were computed by a digital-computer program using inputs from transducer signals. The calculation of simulated oxidant-fuel mass ratios required additional interpretation of the data, because the measured fuel-air and oxygen-air ratios could deviate to a small extent from the exact values for simulation. This meant that a run could have a fuel-air ratio corresponding to a certain simulated O/F and an oxygen-air ratio corresponding to a different simulated O/F. The fuel-air and oxygen-air ratios could always be altered to agree, at a mean simulated O/F, by multiplying the measured air flow by an adjusting factor. This was an arbitrary procedure to be sure, but in this way the nozzle-temperature data could be reported as that corresponding to some mean simulated O/F, with an excess or deficiency of air mass flow. Runs in which this air-flow-adjusting factor turned out to be more than  $\pm 5$  percent from unity were rejected.

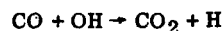
For the calculation of the oxidant-fuel mass ratios, the actual analysis of the fuel mixture was used. The desired fuel analysis as shown in table I gave a molecular weight of 7.08, but it was necessary and economical in handling gaseous fuel mixtures in large quantities to accept a tolerance on the basis of molecular weight of generally  $\pm 4$  percent, occasionally up to 7 percent.

The test of the effectiveness of the simulation technique for the purposes of this study lies in the duplication of the nozzle static temperatures. An example of the sensitivity of these temperatures to deviations from

correct simulation is presented in Fig. 3, which shows static temperature at a nozzle area ratio of 2.05 as a function of simulated oxidant-fuel mass ratio for the two extreme cases of equilibrium and frozen theoretical expansion. Calculated temperatures are shown for the storable propellants and for the simulated propellants, where "off-simulation" is illustrated by: (1) correct composition simulation, but operation at a constant oxidant-inlet temperature of  $1100^{\circ}\text{K}$ , which provides the correct inlet enthalpy only at an O/F of 1.65, (2) incorrect composition simulation caused by an air flow 10 percent high, and (3) incorrect composition simulation caused by a fuel mixture with a molecular weight 7 percent high. The actual simulation conditions were always controlled within the tolerances represented by these curves. Figure 3 shows that the constant oxidant-inlet-temperature case yields temperatures at high O/F values that vary a maximum of  $40^{\circ}\text{K}$  from that for the equilibrium expansion of the storable propellants, and the additional composition discrepancies can alter the temperature by  $100^{\circ}\text{K}$ . For frozen expansion, on the other hand, the storable-propellant and simulated-propellant temperatures are almost indistinguishable. The same results may be calculated at other area ratios beyond the nozzle throat. As shown in the results of this study, the expansion of the storable propellants is near frozen, and the tolerance in operating conditions permitted in this investigation had little influence on temperature profiles.

#### Theoretical Predictions

Figure 3 and subsequent data-presentation figures show theoretical curves calculated from a computer program<sup>(6)</sup> at two extremes requiring no chemical reaction-rate information: equilibrium expansion, in which chemical reaction rates of the exhaust products flowing in the nozzle are infinite, and the recombination reactions are always in chemical equilibrium; and frozen expansion, in which chemical reaction rates are zero, and the composition of the exhaust products is fixed at the equilibrium combustion-chamber-product composition. Of course the actual nozzle expansion proceeds with intermediate chemical reaction rates for the recombination, but an exact kinetic, or finite-rate calculation, can be very complicated and requires a considerable knowledge of chemical reaction rates. It is common to simplify kinetic expansion calculations by using the Bray criterion,<sup>(12)</sup> which assumes equilibrium expansion in the nozzle up to a certain area ratio (the "sudden-freezing" point) and frozen expansion thereafter. The sudden-freezing area ratio is defined as the nozzle location where the rate of decrease of moles of radicals or atoms is equal to the rate of recombination from chemical-kinetic data. This was calculated using the computing method of Franciscus and Healy.<sup>(13)</sup> The principal rate-controlling recombination reactions for the storable propellant system are the three-body reactions presented in table 4 along with the forward reaction-rate constants that were supplied to the simplified computing program of Ref. 13. Previous work on the hydrogen-air system<sup>(3,14)</sup> indicated that reaction (1) was controlling, although reaction (2) and in lean mixtures, reaction (5) may be of importance. It is of interest to note the complete neglect of any carbon or nitrogen reactions; the principal carbon reaction, the water-gas reaction



has an energy release less than 1/4 that of the principal three-body recombination reactions, (1), (2), and (5), and its influence on nozzle temperature can be neglected.<sup>(3,9)</sup>

### Results and Discussion

#### Combustion-Chamber Efficiency

Initial reversal temperature measurements in the combustion chamber showed a flat temperature profile, approximately at the equilibrium combustion temperature. A typical profile has been reported in a previous paper<sup>(9)</sup> for natural gas and air combustion using the same fuel injector and combustion chamber. For practical purposes, combustion efficiency could be considered as 100 percent.

#### Nozzle Temperature Profiles

Some of the experimental static temperatures measured in the test nozzle at a combustion-chamber inlet pressure of 3.7 atmospheres absolute are plotted in Figs. 4(a) to (d) for simulated oxidant-fuel mass ratios of 1.6, 2.0, 2.245, and 2.4. For comparison with the experimental data, the plots show the theoretical equilibrium and frozen-expansion temperatures and the calculations of kinetic expansion based on a "sudden-freezing" analysis for the liquid storable propellants at the indicated O/F.

It is seen that the experimental data and the kinetic curve lie close to the frozen-expansion temperatures. The kinetic calculations indicate a freezing point upstream of the nozzle throat, at an area ratio of about 1.06 for a simulated O/F of 1.6 and at 1.04 for larger ratios, and frozen expansion throughout the supersonic portion of the nozzle. The experimental data fit this simplified kinetic prediction although it was noticed that some of the data indicated a tendency toward temperatures lower than the analysis at the optical stations nearer the throat and somewhat higher temperatures than the analysis at the last optical station. These discrepancies could arise from the usual sources of experimental error, but they can be largely attributed to deviations from one-dimensional flow in the nozzle and shocks. Static-pressure measurements were taken during the tests; and while not presented in this paper, similar deviations from a smooth plot with pressure suggest the presence of weak shocks in the test nozzle.

#### Effect of Oxidant-Fuel Ratio

All of the experimental temperature data have been plotted in Figs. 5(a) to (d) as a function of the corresponding simulated oxidant-fuel mass ratio of the liquid storable propellants. These figures include data at or near the O/F values of Figs. 4(a) to (d) and additional intermediate oxidant-fuel ratio data not included in Figs. 4. The results at the optical station nearest the throat, the area ratio of 1.30, have been omitted from Figs. 5. For reference, Figs. 5(a) to (d) also show the theoretical temperature predictions for equilibrium, frozen, and kinetic expansion of the storable propellants.

It is seen from the experimental data that static

temperature is nearly independent of oxidant-fuel mass ratio for the O/F range between 1.6 and 2.5. If the expansion of the storable propellant followed the equilibrium analysis, the temperature profiles would be clearly O/F dependent, but the experimental data agree with the simplified kinetic calculation for near-frozen expansion, which is generally insensitive to oxidant-fuel ratio.

#### Specific Impulse

The experimental temperature data were used to calculate vacuum specific impulse by linear interpolation between the equilibrium and frozen predictions obtained from the analytical program using the ratio of experimental to theoretical temperatures. No attempts were made to correct for the effect of enthalpy or composition off-simulation, or to allow for combustion and aerodynamic inefficiencies, if any.

The experimental specific impulse and the analytical predictions are plotted in Fig. 6(a) as a function of the storable propellant oxidant-fuel mass ratio, at an area ratio of 3.6. The data are close to the kinetic prediction, falling somewhat below that theoretical curve. It may be noted that at this relatively small area ratio, the peak vacuum specific impulse is attained only at oxidant-fuel ratios below 1.6.

The use of the kinetic analysis for prediction of specific impulse at large area ratios representative of rocket engines is illustrated in Fig. 6(b), which presents theoretical curves for an engine with an area ratio of 60 and a combustion-chamber pressure of 6.8 atmospheres. Representative experimental data from Ref. 1, corrected for combustion and aerodynamic losses to show the effect of kinetic efficiency only, are included in Fig. 6(b). The relative agreement between experimental and predicted specific impulse is very good and resembles the correlation at the lower area ratio in Fig. 6(a).

#### Accuracy of Measurements

An assessment of experimental accuracy would concentrate mainly on the primary measurement instrument, the spectral-line reversal pyrometer. In the range of interest, accuracy and precision of this instrument as noted in the literature<sup>(10)</sup> should be of the order of  $\pm 2$  percent each. Errors due to spatial and temporal fluctuations in the static temperature could add an additional percent or two error.<sup>(11)</sup> At the first optical station in particular, an additional small error may arise from the nonlinear averaging of a radial temperature profile where flow is not one-dimensional. The optical windows were purged with nitrogen to prevent dirtying from condensed combustion products. In a few cases (note the data of Fig. 5(d) near an oxidant-fuel mass ratio of 1.6) subsequent examination of the data revealed temperatures that are too high, possibly due to reduced transmission of the reference lamp radiation.

Oxidant-inlet temperatures were measured by a shielded, aspirated thermocouple with minimum conduction and radiation losses, and the temperatures were corrected for heat losses to the cooled fuel injector. Previous studies with the storage heater showed that the radial temperature profiles were reasonably flat; but because a single thermocouple was used to measure this

temperature, it is believed that oxidant combustion-chamber inlet temperatures were uncertain to  $\pm 5$  percent. Uncertainties of oxidant-inlet temperature of this order should have a negligible effect on the nozzle temperature results. Pressures and flow rates were measured with standard transducers capable of  $\pm 1$  percent accuracy.

#### Concluding Remarks

This paper has presented the results of temperature measurements in a 5.5-area-ratio, nominal Mach 3 nozzle, using hydrogen and methane as fuel and preheated oxygen-enriched air as oxidant to simulate the combustion products and enthalpy of the 50-weight-percent hydrazine and UDMH fuel, nitrogen tetroxide oxidant propellant system.

This use of the conventional gaseous propellants to simulate the liquid storable propellants proved feasible. The flow rates and oxidant-inlet temperatures that were needed to simulate the various oxidant-fuel ratios could be readily calculated but could not always be matched exactly in the experiments. It was, however, calculated that the deviations in exhaust-product composition and enthalpy had little effect on the nozzle static temperatures for the conditions of this study, where the expansion was nearly frozen. For higher combustion-chamber pressures or nozzle geometries that favor expansion nearer to equilibrium, it should be realized that more precise control of the simulation parameters may be necessary.

At 3.7 atmospheres combustion-chamber pressure, over a range of oxidant-fuel mass ratios from 1.6 to 2.5 (equivalence ratios of 1.4 to 0.9), temperatures were nearly independent of oxidant-fuel ratio and were close to those predicted for a frozen expansion. These results are in agreement with a simplified kinetic analysis, using reaction rates for the hydrogen and oxygen three-body recombinations only, which indicated a sudden freezing of the recombination reactions at an area ratio just upstream of the nozzle throat. Results were also interpreted in terms of specific impulse and were applied to higher area ratios typical of advanced rocket engines by using the simplified kinetic analysis.

#### References

1. Aukerman, C. A. and Trout, A. M., "Experimental Rocket Performance of Apollo Storable Propellants in Engines with Large Area Ratio Nozzles," TN D-3566, 1966, National Aeronautics and Space Administration, Cleveland, Ohio.
2. Simkin, D. J. and Koppang, R. R., "Recombination Losses in Rocket Nozzles with Storable Propellants," AIAA Journal, Vol. 1, No. 9, Sept. 1963, pp. 2150-2152.
3. Sarli, V. J., Burwell, W. G., and Zupnik, T. F., "Investigation of Nonequilibrium Flow Effects in High-Expansion-Ratio Nozzles," Report C910096-13 (NASA CR 54221), Dec. 1964, United Aircraft Corp., Research Labs., East Hartford, Conn.

4. Wilde, K. A., "Complex Kinetics in Adiabatic Flow: C-H-O(N) Systems," AIAA Journal, Vol. 3, No. 10, Oct. 1965, pp. 1846-1849.
5. Sheeran, W., "Simulation of Earth-Storable Liquid Propellants with Gaseous Reactants," HFD-PS-67-5, June 1967, Cornell Aero. Labs., Inc., Hypersonic Facilities Dept., Buffalo, N.Y.
6. Zeleznik, F. J. and Gordon, S., "A General IBM 704 or 7090 Computer Program for Computation of Chemical Equilibrium Compositions, Rocket Performance, and Chapman-Jouguet Detonations," TN D-1454, 1962, National Aeronautics and Space Administration, Cleveland, Ohio.
7. McBride, B. J., Heimerl, S., Ehlers, J. G., and Gordon, S., "Thermodynamic Properties to 6000° K for 210 Substances Involving the First 18 Elements," SP-3001, 1963, National Aeronautics and Space Administration, Cleveland, Ohio.
8. Lezberg, E. A. and Lancashire, R. B., "Expansion of Hydrogen-Air Combustion Products Through a Supersonic Exhaust Nozzle. Measurement of Static-Pressure and Temperature Profiles," Combustion and Propulsion, Fourth AGARD Colloquium, Pergamon Press, New York, 1961, pp. 286-305.
9. Lezberg, E. A. and Franciscus, L. C., "Effects of Exhaust Nozzle Recombination on a Hypersonic Ramjet Performance: I. Experimental Measurements," AIAA Journal, Vol. 1, No. 9, Sept. 1963, pp. 2071-2076.
10. Buchele, D., "A Self-Balancing Line-Reversal Pyrometer, Temperature, Its Measurement and Control in Science and Industry," Vol. 3, Part 2, Reinhold Publ. Co., New York, 1962, pp. 879-887.
11. Lezberg, E. A. and Buchele, D., "Some Optical Techniques for Temperature and Concentration Measurements of Combustion in Supersonic Streams," Paper 64-536, May 1964, AIAA, New York.
12. Bray, K. N. C., "Atomic Recombination in a Hypersonic Wind-Tunnel Nozzle," Journal of Fluid Mechanics, Vol. 6, 1959, pp. 1-32.
13. Franciscus, L. C. and Healy, J. A., "Computer Program for Determining Effects of Chemical Kinetics on Exhaust Nozzle Performance," TN D-4144, 1967, National Aeronautics and Space Administration, Cleveland, Ohio.
14. Lezberg, E. A., Rose C. M., and Friedman, R., "Comparisons of Experimental Hydroxyl Radical Profiles with Kinetic Calculations in a Supersonic Nozzle," TN D-2883, 1965, National Aeronautics and Space Administration, Cleveland, Ohio.
15. Getzinger, R. W. and Schott, G. L., "Kinetic Studies of Hydroxyl Radicals in Shock Waves. V. Recombination via the  $H + O_2 + M \rightarrow HO_2 + M$  Reaction in Lean Hydrogen-Oxygen Mixtures," Journal of Chemical Physics, Vol. 43, No. 9, Nov. 1, 1965, pp. 3237-3247.
16. Strehlow, R. A. and Rubins, P. M., "Experimental and Analytical Study of the Hydrogen-Air Reaction Kinetics Using a Standing-Wave Normal Shock," Paper 67-479, July 1967, AIAA, New York.

Constituent	Volume percent
Hydrogen	66.80
Methane	30.75
Ethane	1.13
Carbon dioxide	.49
Helium	.35
Nitrogen	.25
Propane	.19
Butanes and higher hydrocarbons	.04
	100.00

TABLE I. - TYPICAL ANALYSIS OF HYDROGEN AND NATURAL GAS FUEL MIXTURE



Storable propellants			Simulated propellants		
Constituent and volume percent	State and temperature, °K	Enthalpy, cal/mole	Constituent and volume percent	State and temperature, °K	Enthalpy, cal/mole
Fuel					
N <sub>2</sub> H <sub>4</sub> , 65.2	Liq., 298	12050	H <sub>2</sub> , 66.80	Gas, 298	0
C <sub>2</sub> H <sub>8</sub> N <sub>2</sub> , 34.8	Liq., 298	12734	CH <sub>4</sub> , 30.75	Gas, 298	-17899
			C <sub>2</sub> H <sub>6</sub> , 1.13	Gas, 298	-20236
(Additional minor constituents omitted)					
Oxidant					
N <sub>2</sub> O <sub>4</sub> , 100	Liq., 298	-6873	N <sub>2</sub> , (Composition varies with O/F)	Gas, 298	0
			O <sub>2</sub>	Gas, 298	0
			N <sub>2</sub>	Gas, 950	4743
			O <sub>2</sub>	Gas, 950	5013

TABLE II. - ENTHALPY OF REACTANTS

Properties	Storable propellants		Simulated propellants at 1100° K oxidant-inlet temperature	
	At combustion chamber	At nozzle exit for expansion to 1/30 P <sub>c</sub>	At combustion chamber	At nozzle exit for expansion to 1/30 P <sub>c</sub>
Nozzle-exit-to-throat area ratio	-----	4.892	-----	4.898
Temperature, °K	2992	1850	2991	1853
Enthalpy, cal/g	67.1	-720.8	61.2	-724.9
Specific heat ratio	1.140	1.234	1.139	1.234
Mach number	0	2.710	0	2.715
Vacuum specific impulse	-----	290.6	-----	290.3
Composition, mole fractions				
He	0.0000	0.0000	0.0013	0.0014
CO	.0973	.0827	.0961	.0813
CO <sub>2</sub>	.0337	.0531	.0343	.0540
H	.0294	.0006	.0290	.0006
H <sub>2</sub>	.1365	.1473	.1330	.1430
H <sub>2</sub> O	.3441	.3788	.3456	.3813
O	.0033	.0000	.0034	.0000
O <sub>2</sub>	.0033	.0000	.0035	.0000
N <sub>2</sub>	.3233	.3373	.3243	.3384
NO	.0039	.0000	.0041	.0000
OH	.0251	.0001	.0255	.0001
Molecular weight	20.48	21.23	20.54	21.30

TABLE III. - COMPARISON OF CALCULATED PROPERTIES AND COMPOSITIONS  
[Oxidant-fuel mass ratio, 1.6; combustion-chamber pressure, P<sub>c</sub>, 3.7 atm abs.]

Reaction number	Reaction <sup>a</sup>	Forward reaction rate constant, $k_f$ , (°K)(cm <sup>6</sup> )/(mole <sup>2</sup> )(sec)	Source
1	$H + OH + M \rightarrow H_2O + M$	$7.50 \times 10^{19}$	Ref. 9
2	$H + H + M \rightarrow H_2 + M$	$0.30 \times 10^{19}$	Ref. 9
3	$O + O + M \rightarrow O_2 + M$	$0.995 \times 10^{19}$	Ref. 9
4	$H + O + M \rightarrow OH + M$	$0.40 \times 10^{19}$	Ref. 4
5	$H + O_2 + M \rightarrow HO_2 + M$	$2.74 \times 10^{19}$	Ref. 15, with third-body efficiencies adapted from those reported by Ref. 16

<sup>a</sup> M is any third body.

TABLE IV. - RECOMBINATION REACTIONS AND THEIR FORWARD RATES USED IN THE SIMPLIFIED KINETIC EXPANSION ANALYSE

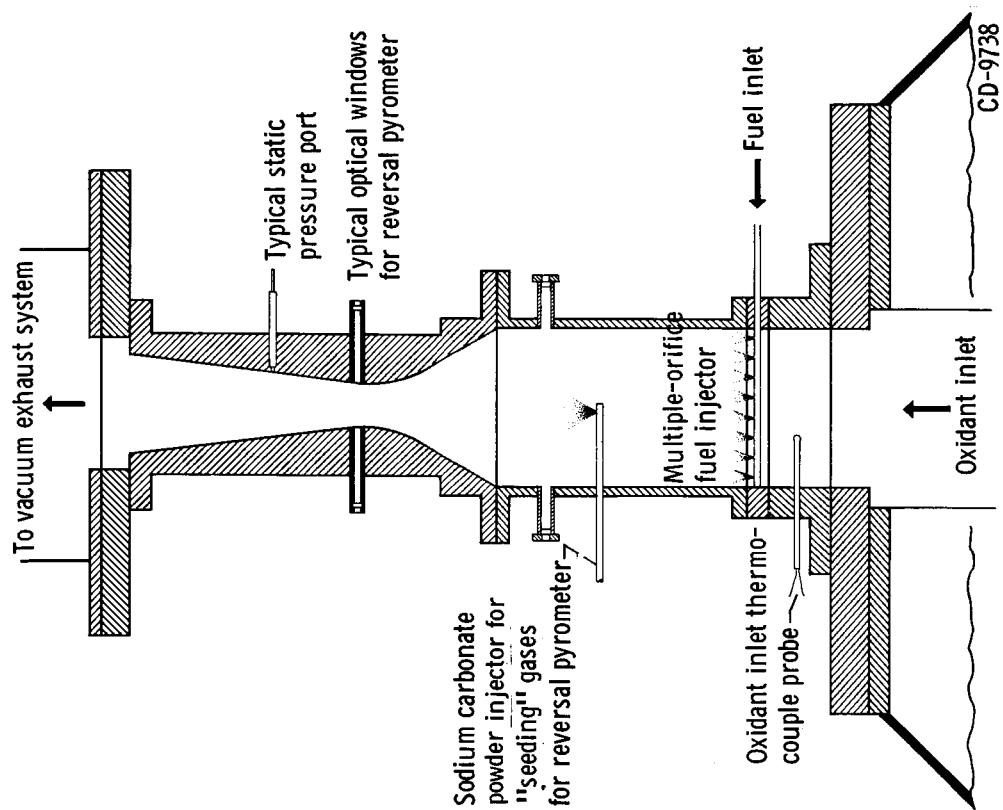


Figure 2. - Sketch of combustion chamber and test nozzle.

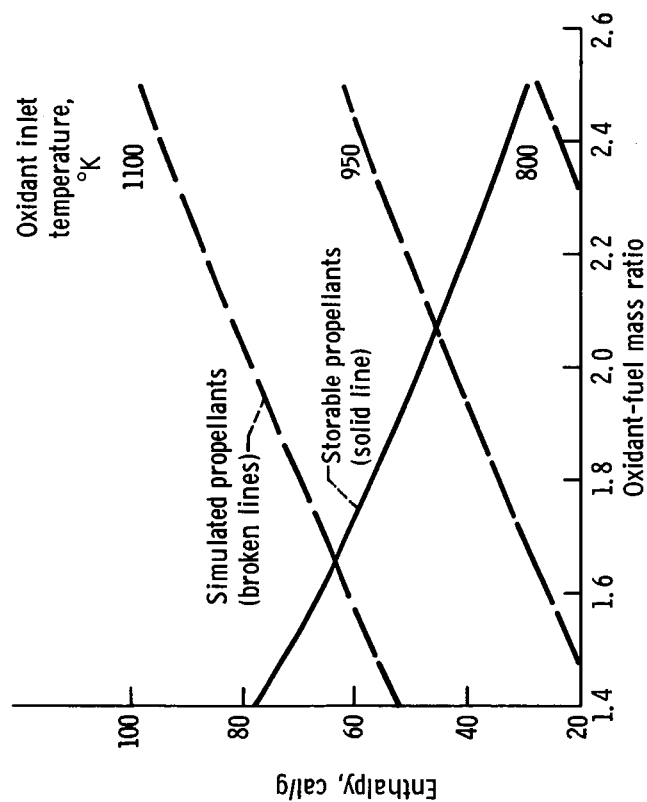


Figure 1. - Calculated enthalpy of combustion products at 3.7 atmospheres.

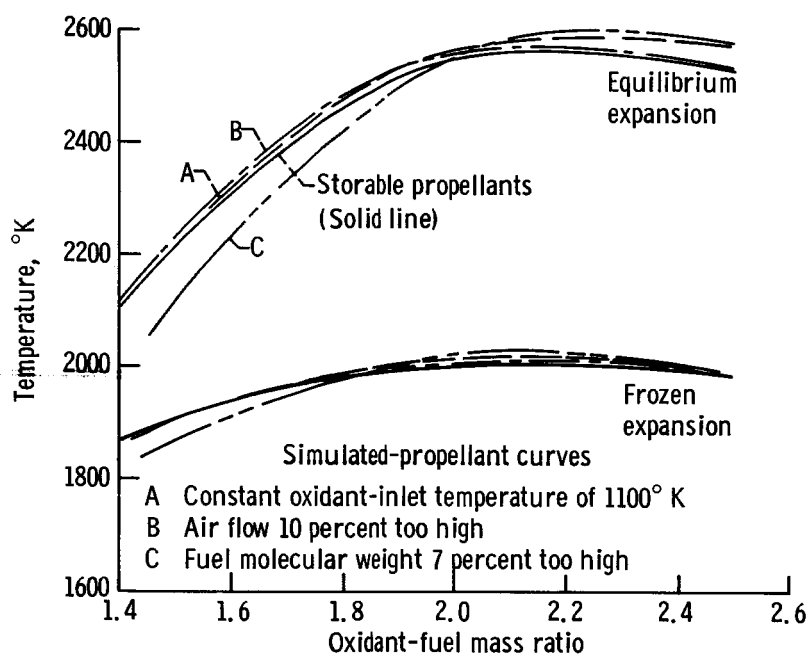
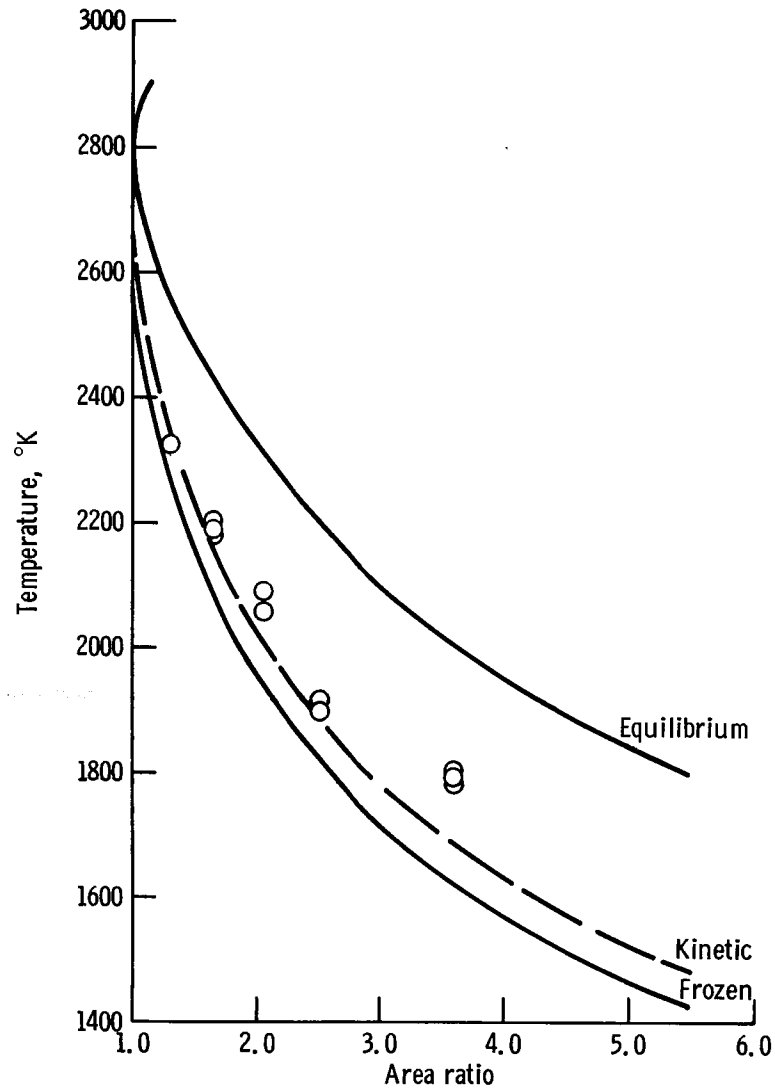
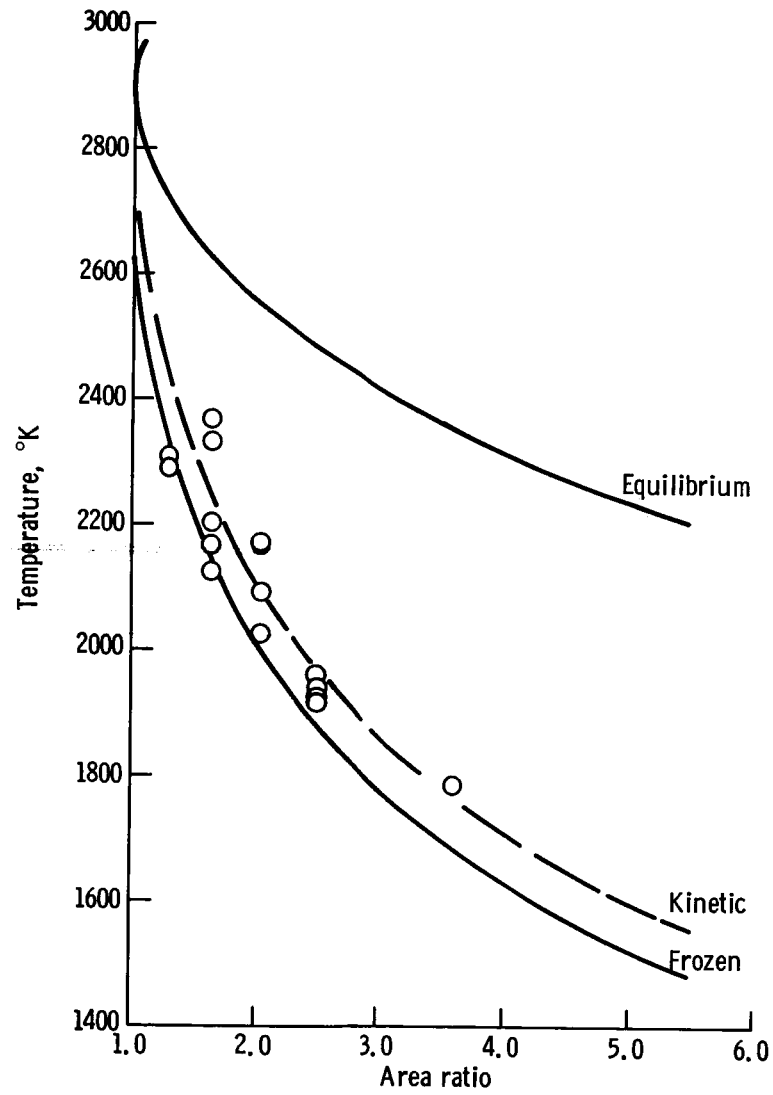


Figure 3. - Effect of simulation conditions on nozzle static temperature. Area ratio, 2.05; pressure, 3.7 atmospheres.



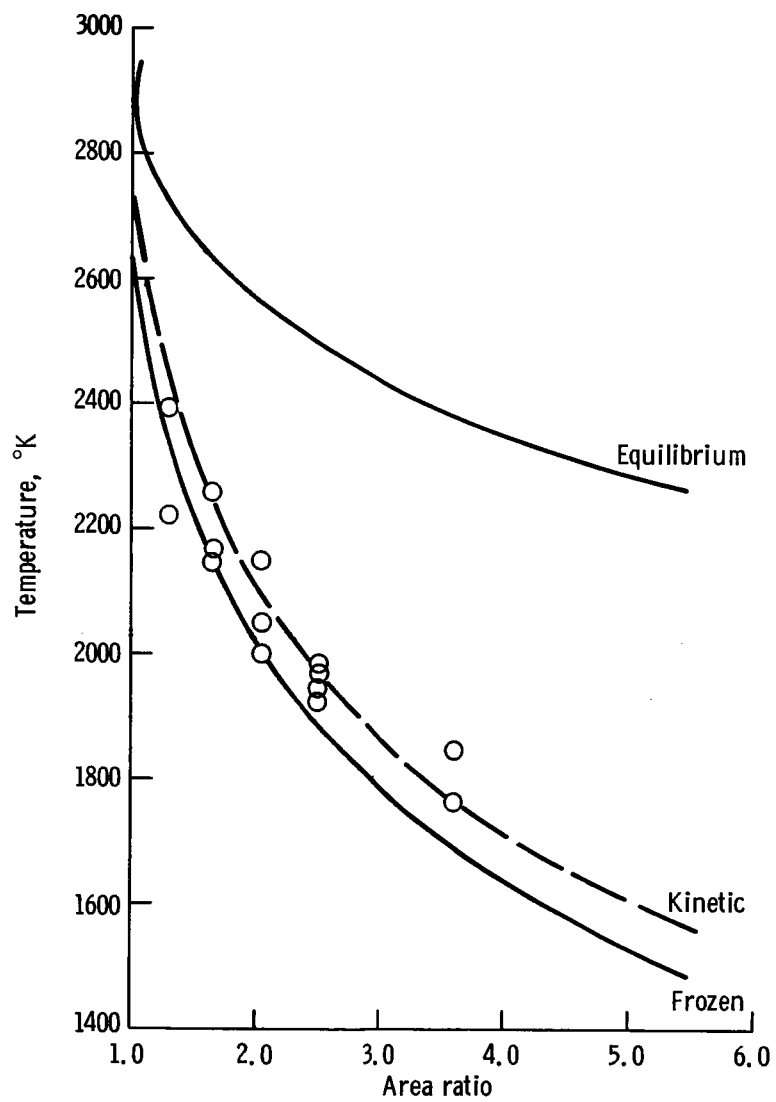
(a) Oxidant-fuel mass ratio, 1.6.

Figure 4. - Nozzle static temperatures at 3.7 atmospheres combustion-chamber pressure. Experimental points for simulated propellants; theoretical curves for storable propellants



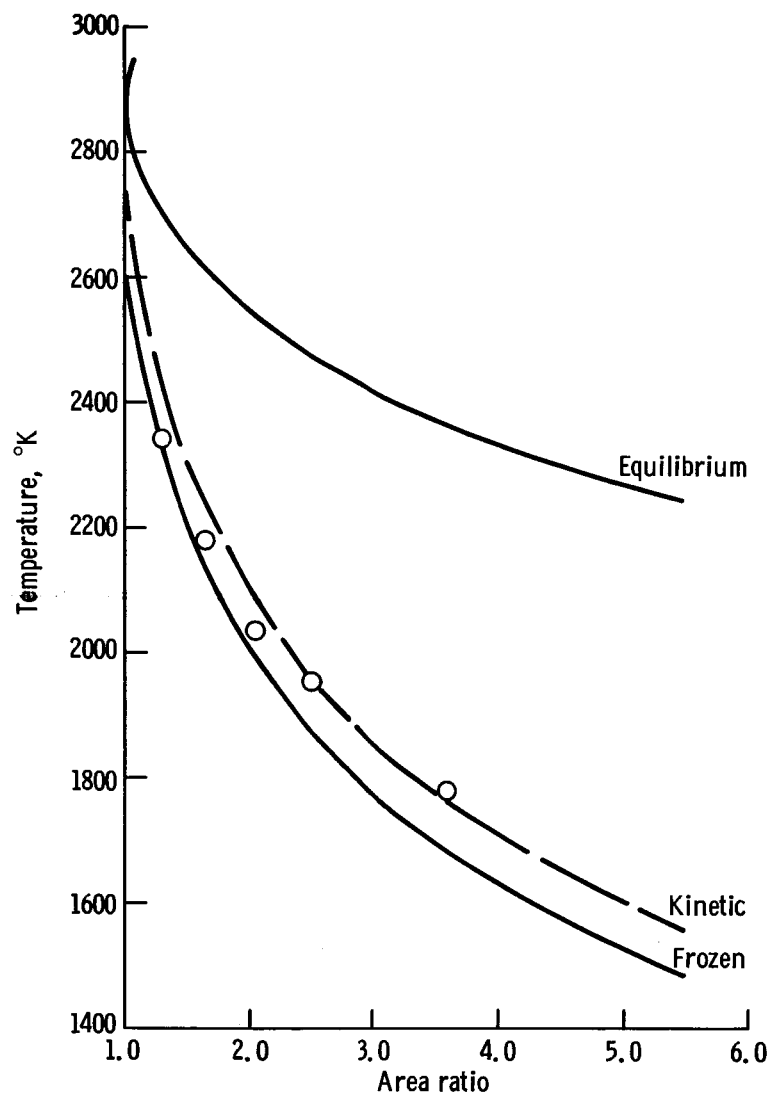
(b) Oxidant-fuel mass ratio, 2.0.

Figure 4. - Continued.



(c) Oxidant-fuel mass ratio, 2.245.

Figure 4. - Continued.



(d) Oxidant-fuel mass ratio, 2.4.

Figure 4. - Concluded.



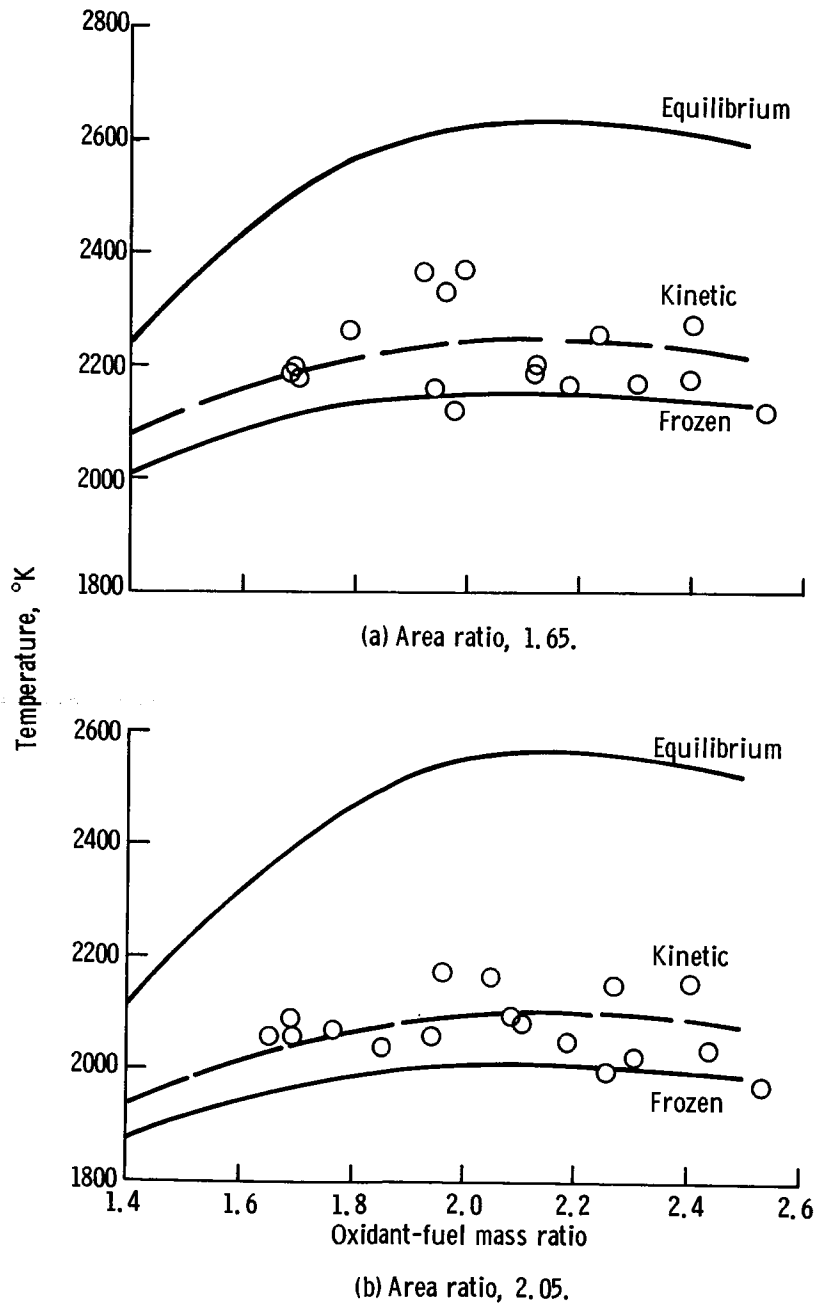


Figure 5. - Effect of oxidant-fuel mass ratio on nozzle static temperature at 3.7 atmospheres combustion-chamber pressure. Experimental points for simulated propellants; theoretical curves for storable propellants.

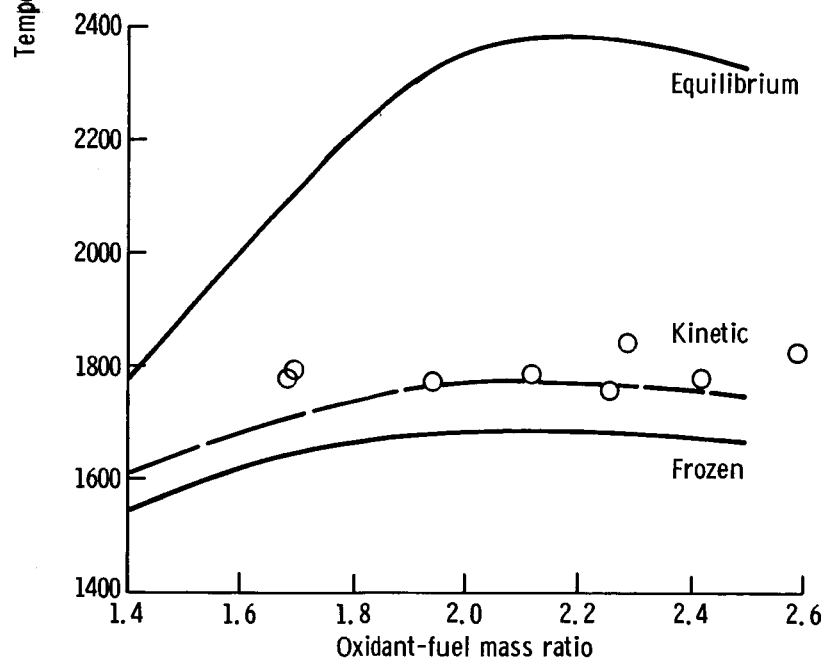
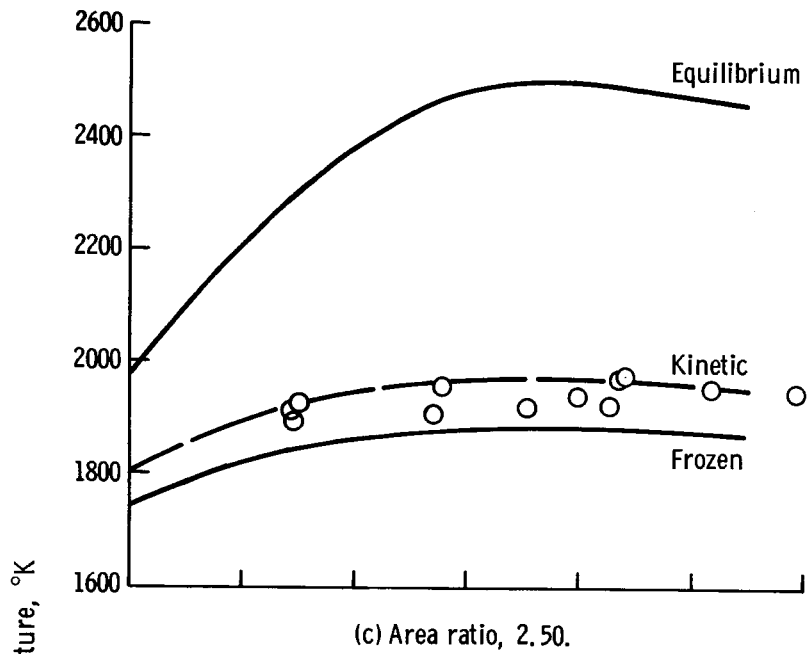
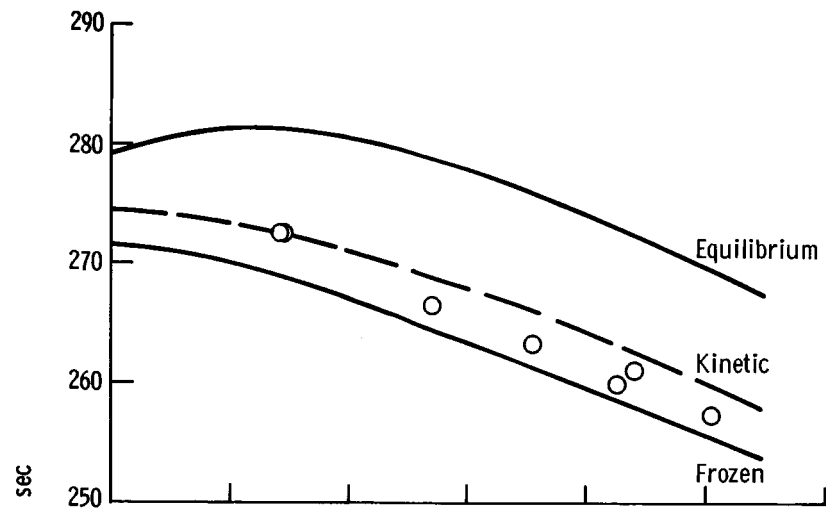
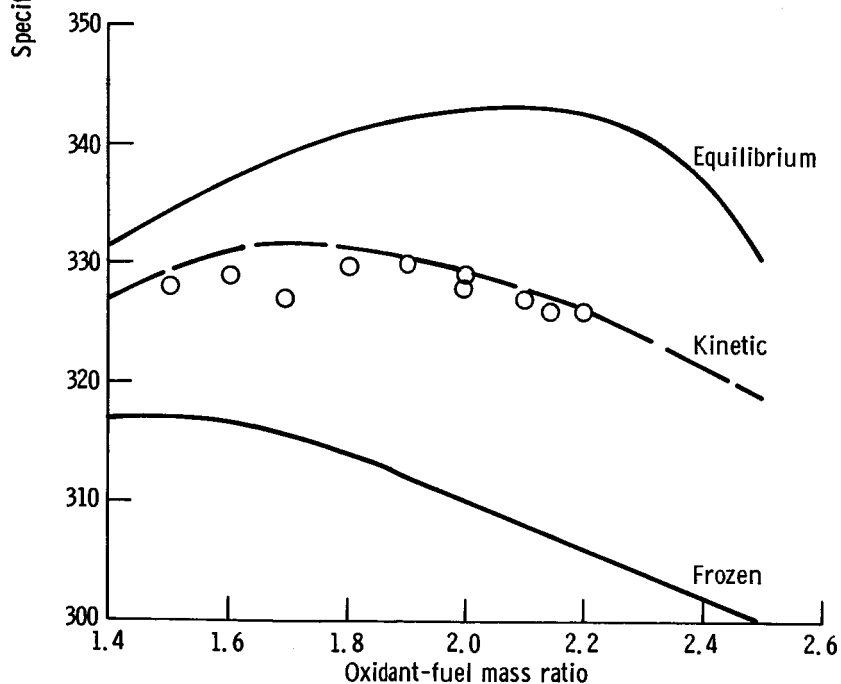


Figure 5. - Concluded.



(a) This study. Area ratio, 3.60; combustion-chamber pressure, 3.7 atmospheres. Experimental points for simulated propellants; theoretical curves for storable propellants.



(b) Data of reference 1. Area ratio, 60.0; combustion-chamber pressure, 6.8 atmospheres. Experiment and theory for storable propellants.

Figure 6. - Vacuum specific impulse.